THE JOURNAL OF PHYSICAL CHEMISTRY B LETTERS

2005, *109,* 11862−11864
Published on Web 05/26/2005

Molecular Simulation of Adsorption and Diffusion of Hydrogen in Metal−Organic Frameworks

Qingyuan Yang and Chongli Zhong*

Department of Chemical Engineering, Beijing University of Chemical Technology, Beijing 100029, China

Received: April 13, 2005; In Final Form: May 9, 2005

Metal−organic frameworks (MOFs) are thought to be a set of promising hydrogen storage materials; however, little is known about the interactions between hydrogen molecules and pore walls as well as the diffusivities of hydrogen in MOFs. In this work, we performed a systematic molecular simulation study on the adsorption and diffusion of hydrogen in MOFs to provide insight into molecular-level details of the underlying mechanisms. This work shows that metal−oxygen clusters are preferential adsorption sites for hydrogen in MOFs, and the effect of the organic linkers becomes evident with increasing pressure. The hydrogen storage capacity of MOFs is similar to carbon nanotubes, which is higher than zeolites. Diffusion of hydrogen in MOFs is an activated process that is similar to diffusion in zeolites. The information derived in this work is useful to guide the future rational design and synthesis of tailored MOF materials with improved hydrogen adsorption capability.

Hydrogen is well-recognized as a future energy carrier; however, its application in vehicles and portable electronics as an energy carrier is limited by hydrogen storage problems. Although various materials have been studied as hydrogen storage materials, none is capable of meeting the U.S. DOE cost and performance targets. Metal−organic frameworks (MOFs) are thought to be a set of promising hydrogen storage materials,[1−4] and various MOFs have been synthesized and characterized for their hydrogen storage capacities.[5−10] However, little is known about the interactions between H_2 molecules and pore walls, as well as the diffusivities of H_2 in MOFs, for which molecular modeling is a powerful tool to provide insight into molecular-level details of the underlying mechanisms that can guide the future rational design and synthesis of tailored MOF materials with significantly improved H_2 adsorption capability. Although several molecular simulations have been performed,[11−15] simulation studies on H_2 in MOFs are vary scarce. Therefore, in this work, we perform a systematic molecular simulation study on the adsorption and diffusion of H_2 in MOFs, and the isoreticular metal−organic frameworks (IRMOFs) synthesized by Eddaoudi et al.[16] are adopted as a representative of MOFs. Since most MOFs that behave as hydrogen storage materials have similar chemical structures, consisting of metal−oxygen bonded units and organic units, the knowledge obtained from IRMOFs is expected to apply to a broad range of MOFs.

To study the mechanism of hydrogen adsorption in MOFs, adsorption isotherms of H_2 in IRMOFs-1, -8, and -18 (see Figure 1) were simulated with grand canonical Monte Carlo (GCMC) simulations[17,18] (see Supporting Information). The H_2 molecule was modeled as a two-site Lennard-Jones (LJ) molecule with the parameters obtained in this work by fitting the experimental *PVT* curve of bulk H_2 and validated with H_2 bulk diffusion data (see Supporting Information). The interactions of H_2 molecules with the atoms of the IRMOFs were described by the all-atom OPLS force field (OPLS-AA).[19] To better represent the experimental adsorption isotherms of H_2 in IRMOFs,[7] the energy parameters of the OPLS-AA force field for oxygen, methyl hydrogen, and carbon were refitted (see Supporting Information). The simulated and experimental isotherms of H_2 in IRMOFs-1 and -18 at 77 K are shown in Figure 2a. Obviously, the force fields employed give good agreement between simulation and experiment.

Recently, Sagara et al. performed GCMC simulations of the adsorption isotherms of H_2 in IRMOF-1 using the standard universal force field (UFF).[14] Their results are also depicted in Figure 2a for comparison. Evidently, their method gives systematically higher adsorption capacities than experimental observations. This also illustrates the necessity of employing an alternative force field in this work with some refined parameters to better represent the adsorption isotherms of H_2 in IRMOFs.

To study the effects of organic linkers on H_2 adsorption, simulations were further performed on IRMOF-8 at $P = 0-10$ MPa, and the results are shown in Figure 2b, in which the simulated results for IRMOFs-1 and -18 in the same pressure range are also given for comparison. Obviously, IRMOF-8 shows similar H_2 storage capacity to IRMOF-1 at low pressures, and the difference becomes evident at high pressures. IRMOF-18, however, always shows lower H_2 storage capacity than both of them in the whole pressure range. This can be explained clearly if we refer to the snapshots of the structures of IRMOF-1 with adsorbed H_2 at various pressures, as given in Figure 3.

Figure 3 shows that the mechanism of hydrogen adsorption in IRMOFs is as follows: H_2 molecules first occupy the corner regions, and the organic units start adsorbing H_2 molecules at high pressures, followed by the filling of the inner spaces of the cavities. This is consistent with the experimental observa-

* Corresponding author. Email: zhongcl@mail.buct.edu.cn.

10.1021/jp051903n CCC: $30.25

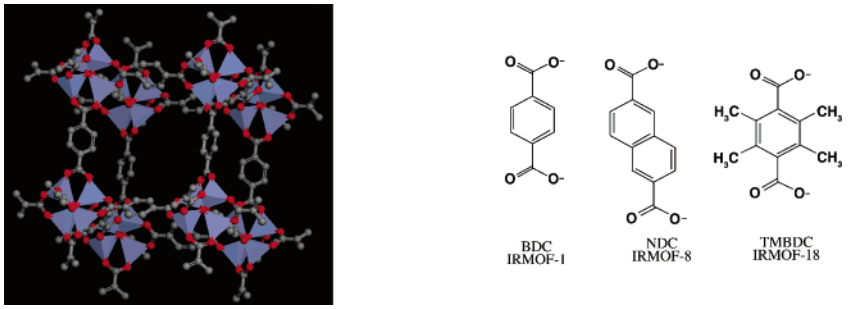

Figure 1. Unit-cell crystal structure of IRMOFs, $Zn_4O(L)_3$. On each of the corners is a cluster $[OZn_4(CO_2)_6]$ of an oxygen-centered Zn_4 tetrahedron that is bridged by six carboxylates of an organic linker (Zn, blue polyhedron; O, red spheres; C, gray spheres).

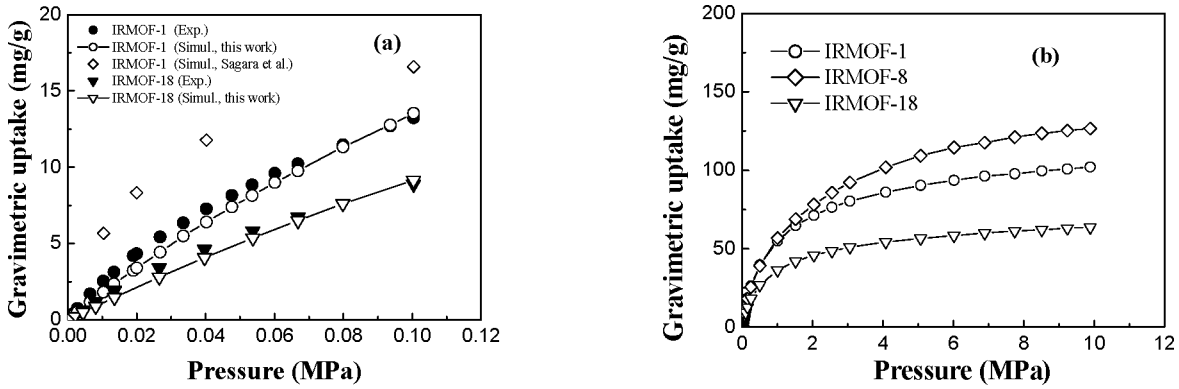

Figure 2. (a) Comparison of simulated and experimental isotherms for IRMOFs-1 and -18 at 77 K. (b) Comparison of simulated isotherms of IRMOFs-1, -8, and -18 at 77 K and $P = 0-10$ MPa.

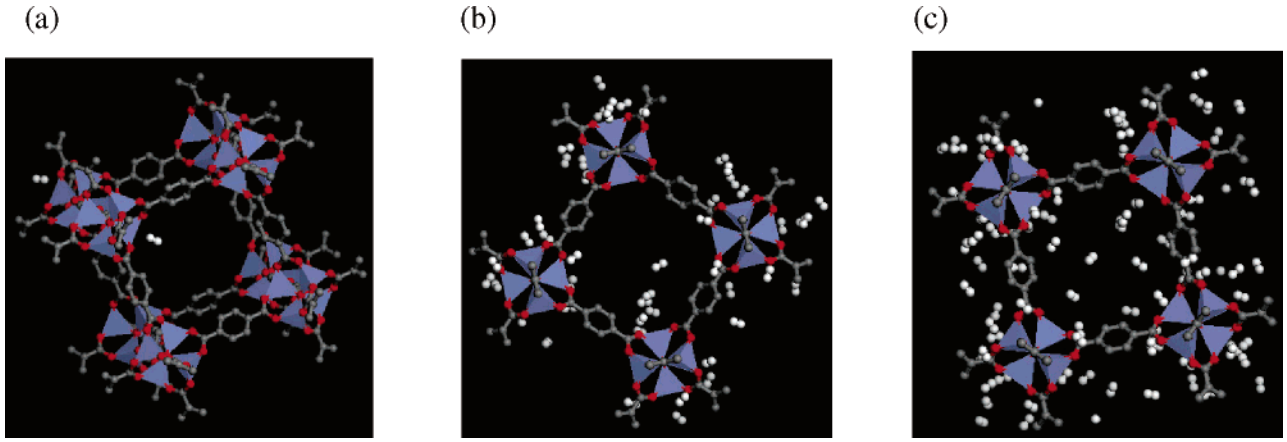

Figure 3. Snapshots of the structures of IRMOF-1 with adsorbed H_2 at various pressures: (a) $P = 0.0028$ MPa, (b) $P = 0.1$ MPa, and (c) $P = 0.25$ MPa (Zn, blue polyhedron; O, red spheres; C, gray spheres; H, white spheres).

tions of Rosi et al.[5] and Kubota et al.,[9] who concluded that the metal−oxygen unit is the most preferential H_2 adsorption site in MOFs. On the basis of the above H_2 adsorption mechanism, at low pressures (low H_2 loadings), only Zn−O units are adsorption sites, and thus, IRMOF-8 has similar adsorption capacity to IRMOF-1; while at high pressures (high H_2 loadings), organic units start adsorbing H_2, leading to a higher adsorption capacity for IRMOF-8 over IRMOF-1. As for IRMOF-18, both the experimental and simulated results show that its storage capacity is smaller than that of IRMOF-1. This may be attributed to the steric hindrance effects caused by the pendant groups adorning the phenylene spacer on the adsorption of H_2 molecules at the corners, and thus, such groups should be avoided in designing new materials.

The studies on H_2 uptake at 77 K and 0.1 MPa show that MOFs have similar H_2 storage capacity to carbon nanomaterials,[20] which is much higher than that of the most favorable zeolite ZSM-5 (0.7 wt %). An examination of our simulated excess adsorption isotherms at 77 K suggests that 26 H_2, 35 H_2, and 20 H_2 per formula unit are close to adsorption saturation for IRMOFs-1, -8, and -18, respectively.

The diffusivity of H_2 in MOFs is an important property; however, to date no knowledge about this is known. Therefore, constant-temperature equilibrium molecular dynamics (MD) simulations were performed to calculate the self-diffusivity D_s of H_2 in IRMOFs-1, -8, and -18 as a function of pressure (see Supporting Information), as shown in Figure 4.

Obviously, the diffusion of H_2 in IRMOF-18 is much slower than diffusion in the other two materials, which is mainly caused by the steric hindrance effects of the pendant CH_3 groups. On the other hand, H_2 molecules diffuse more rapidly in IRMOF-8 than that in IRMOF-1 because of the relatively larger pore size in the former. Around 100 K, the self-diffusion coefficients of H_2 in various zeolites at low pressure were found experimentally

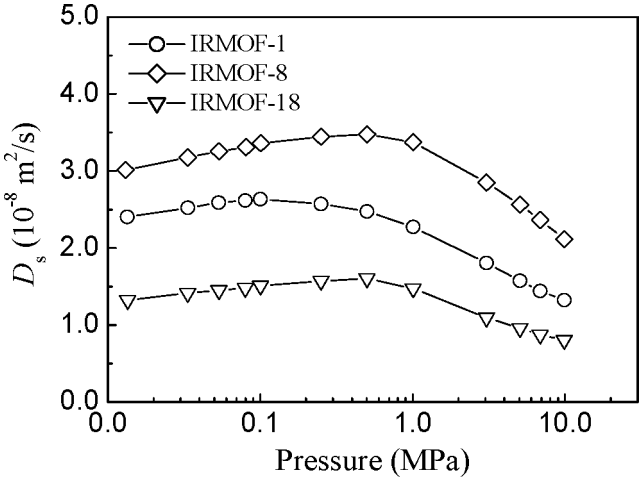

Figure 4. The dependence of self-diffusivity of hydrogen on pressure at $T = 77$ K.

to be around 0.1−1 (10^{-8} m^2/s);[21,22] thus, it seems that the diffusivity of H_2 in MOFs is slightly larger than in zeolites. The dependence of the self-diffusivity of H_2 on pressure in the three IRMOFs shows the same trend (see Figure 4), that is, it first increases with increasing pressure then decreases with further increasing pressure. This phenomena can be explained in the following manner: At low pressures (low H_2 loadings), H_2 molecules are adsorbed at the corners, and the large adsorption energies of the corners lead to low H_2 diffusivities; at higher pressures (higher H_2 loadings), H_2 molecules are also adsorbed at the organic linkers, and the relatively smaller adsorption energies of the organic linkers as compared to the corners lead to an increase in H_2 diffusivities; at even higher pressures, steric hindrance effects cause a lowering of the H_2 diffusivities.

Diffusion of H_2 in IRMOFs was found to be an activated process, as in zeolites. The infinite-dilution activation energies for the self-diffusion of H_2 in IRMOFs-1, -8, and -18 were calculated by performing MD simulations at three temperatures: $T = 77$, 120, and 160 K. The values obtained are 2.55, 2.10, and 3.09 kJ/mol, respectively. The activation energy of H_2 in zeolite NaX was found experimentally to be 4.0 kJ/mol,[22] and it is 1.12 kJ/mol for single-walled carbon nanotubes.[23] Thus, the activation energy for diffusion in MOFs is similar to that in zeolites and carbon nanotubes.

In summary, this work shows that metal−oxygen clusters are preferential adsorption sites for H_2 in MOFs, and the effect of the organic linkers becomes evident with increasing pressure. The H_2 storage capacity of MOFs is similar to that of carbon nanotubes, which is much higher than zeolites. Furthermore, diffusion of H_2 in MOFs is an activated process that is similar to diffusion in zeolites. Finally, it should be pointed out that, although this work demonstrates that IRMOFs are promising hydrogen storage materials that can store a huge amount of H_2 at 77 K, their suitability as practical H_2 storage materials should be evaluated further at the conditions of room temperature and moderate pressure. This work is underway now in our group.

Acknowledgment. The financial support of the Natural Science Foundation of China (contract 20476003) and the Specialized Research Fund for the Doctoral Program of Higher Education of China (contract 20040010002) are greatly appreciated.

Supporting Information Available: Simulation details, force field parameters, and the validation of force fields and simulation programs. This material is available free of charge via the Internet at http://pubs.acs.org.

References and Notes

(1) Noro, S.; Kitagawa, S.; Kondo, M.; Seki, K. *Angew. Chem., Int. Ed.* **2000**, *39*, 2082−2084.
(2) Rosseinsky, M. J. *Microporous Mesoporous Mater.* **2004**, *73*, 15−30.
(3) Rowsell, J. L. C.; Yaghi, O. M. *Microporous Mesoporous Mater.* **2004**, *73*, 3−14.
(4) Snurr, R. Q.; Hupp, J. T.; Nguyen, S. T. *AIChE J.* **2004**, *50*, 1090−1095.
(5) Rosi, N. L.; Eckert, J.; Eddaoudi, M.; Vodak, D. T.; Kim, J.; O'Keeffe, M.; Yaghi, O. M. *Science* **2003**, *300*, 1127−1129.
(6) Foster, P. M.; Eckert, J.; Chang, J.; Park, S.; Férey, G.; Cheetham, A. K. *J. Am. Chem. Soc.* **2003**, *125*, 1309−1312.
(7) Rowsell, J. L. C.; Millward, A. R.; Park, K. S.; Yaghi, O. M. *J. Am. Chem. Soc.* **2004**, *126*, 5666−5667.
(8) Pan, L.; Sander, M. B.; Huang, X.; Li, J.; Smith, M.; Bittner, E.; Bockrath, B.; Johnson, J. K. *J. Am. Chem.* Soc. **2004**, *126*, 1308−1309.
(9) Kubota, Y.; Takata, M.; Matsuda, R.; Kitaura, R.; Kitagawa, S.; Kato, K.; Sakata, M.; Kobayashi, T. C. *Angew. Chem., Int. Ed.* **2005**, *44*, 920−923.
(10) Kesanli, B.; Cui, Y.; Smith, M. R.; Bittner, E. W.; Bockrath, B. C.; Lin, W. *Angew. Chem., Int. Ed.* **2005**, *44*, 72−75.
(11) Vishnyakov, A.; Ravikovitch, P. I.; Neimark, A. V.; Bülow, M.; Wang, Q. M. *Nano Lett.* **2003**, *3*, 713−718.
(12) Düren, T.; Sarkisov, L.; Yaghi, O. M.; Snurr, R. Q. *Langmuir* **2004**, *20*, 2683−2689.
(13) Skoulidas, A. I. *J. Am. Chem. Soc.* **2004**, *126*, 1356−1357.
(14) Sagara, T.; Klassen, J.; Ganz, E. *J. Chem. Phys.* **2004**, *121*, 12543−12547.
(15) Düren, T.; Snurr, R. Q. *J. Phys. Chem. B* **2004**, *108*, 15703−15709.
(16) Eddaoudi, M.; Kim, J.; Rosi, N.; Vodak, D.; Wachter, J.; O'Keeffe, M.; Yaghi, O. M. *Science* **2002**, *295*, 469−472.
(17) Frenkel, D.; Smit, B. *Understanding Molecular Simulation*: *From Algorithms to Applications*; Academic Press: San Diego, 2002.
(18) Yang, Q.; Bu, X.; Zhong, C.; Li, Y.-G. *AIChE J.* **2005**, *51*, 281−291.
(19) Jorgensen, W. L.; Maxwell, D. S.; Tirado-Rives, J. *J. Am. Chem. Soc.* **1996**, *118*, 11225−11236.
(20) Schimmel, H. G.; Kearley, G. J.; Nijkamp, M. G.; Visser, C. T.; de Jong, K. P.; Mulder, F. M. *Chem.—Eur. J.* **2003**, *9*, 4764−4770.
(21) Jobic, H.; Kärger, J.; Bée, M. *Phys. Rev. Lett.* **1999**, *82*, 4260−4263.
(22) Bär, N.-K.; Ernst, H.; Jobic, H.; Kärger, J. *Magn. Reson. Chem.* **1999**, *37*, S79−S83.
(23) Narehood, D. G.; Pearce, J. V.; Eklund, P. C.; Sokol, P. E.; Lechner, R. E.; Pieper, J.; Copley, J. R. D.; Cook, J. C. *Phys. Rev. B* **2003**, *67*, 205409.